Biol. Cybern. 75, 239–251 (1996)

Biological Cybernetics

A neural network model for stroboscopic alternative motion

Hans-Otto Carmesin, Stefan Arndt

Department of Theoretical Neurophysics and Center for Cognitive Sciences, University of Bremen, D-28334 Bremen, Germany

Received: 13 September 1995 / Accepted: 3 June 1996

Abstract. A neural network which models multistable perception is presented. The network consists of sensor and inner neurons. The dynamics is established by a stochastic neuronal dynamics, a formal Hebb-type coupling dynamics and a resource mechanism that corresponds to saturation effects in perception. From this a system of coupled differential equations is derived and analyzed. Single stimuli are bound to exactly one percept, even in ambiguous situations where multistability occurs. The network exhibits discontinuous as well as continuous phase transitions and models various empirical findings, including the percepts of succession, alternative motion and simultaneity; the percept of oscillation is explained by oscillating percepts at a continuous phase transition.

1 Introduction

The investigation of perception, that is of the transformation of a configuration of physical stimuli into one psychological percept by the nervous system, has a long tradition. For instance, Descartes suggested topologically correct organization of stimuli in the brain (Descartes 1664; Corsi 1991) and Necker studied ambiguous perception of drawings of cubes (Necker 1832). In general, the investigation of ambiguous and illusionary percepts has become a fruitful scientific approach in psychology and physiology (see for instance Köhler 1920; Metzger 1975; Kruse 1988; Hock et al. 1993; Basar-Eroglu et al. 1993).

The present investigation continues studies based on very simple stimulus sequences that give rise to motion percepts (Ditzinger and Haken 1989; Kruse et al. 1991; Hock et al. 1993; Basar-Eroglu et al. 1993; Carmesin 1994b). A common feature of such stimulations is that the emergence of percepts exhibits properties of phase transitions, such as multistability and hysteresis. In general, such phase transitions may be characterized by order parameters and by the susceptibility with which order parameter changes can be induced by small additional external stimuli. Such susceptibilities may become very large or may even diverge at particular parameter constellations, for instance at a continuous phase transition, as indicated by a neural network (Carmesin 1994a). As yet these perceptions have not been investigated systematically at such singular conditions. Accordingly, a group of psychologists developed stimulus sequences that give rise to such singular perception conditions (Kruse et al. 1996). In the present paper, a corresponding network model, based on a general field theory (Carmesin 1994a, 1995) is proposed and analyzed.

As a result, it is shown how the high susceptibility together with an 'attention adaptation' give rise to novel phenomena such as oscillation percepts, so-called fluttering; how the area of the hysteresis loop varies; how the empirical data can be explained quantitatively in terms of neuronal network parameters and resulting order parameters corresponding to 'Hebb cell assemblies'; how the same neuronal network models electroencephalographic (EEG) data (Basar-Eroglu et al. 1993; Carmesin 1994a,b); and how the same neuronal network might model neuropharmacological experiments currently being prepared concerning the physiological basis of fast stimulus binding during perception.

Correspondence to: S. Arndt

2 External stimulations

Perception always provides the binding of single stimuli. Such stimulus binding may be especially simple in the case of binding stimulus sequences to motion percepts. A very simple example of such stimulation is provided by a light dot alternating stroboscopically with some frequency ν on a computer screen (Kruse et al. 1991) (Fig. 1). At very low frequency, a human observer perceives the successive positions of the dot, so-called *succession*. At intermediate frequency, an observer perceives a moving dot, a so-called *motion percept*; in particular, this is so-called *stroboscopic motion* (SM). At high frequency, an observer perceives two simultaneously illuminated dots, so-called *simultaneity*.

Such dots may be combined to form larger patterns in order to study novel phenomena. Here, two such combinations are analyzed, both of which give rise to the additional phenomenon of two bistable motion percepts, rather than one monostable motion percept. Accordingly, the motion percepts that arise are called *stroboscopic alternative motions*.

Fig. 1. Stroboscopic stimulation. *Abscissa*, time. *Ordinate*, taken pattern μ. Frequency ν is equal to the inverse period of periodic stimulation

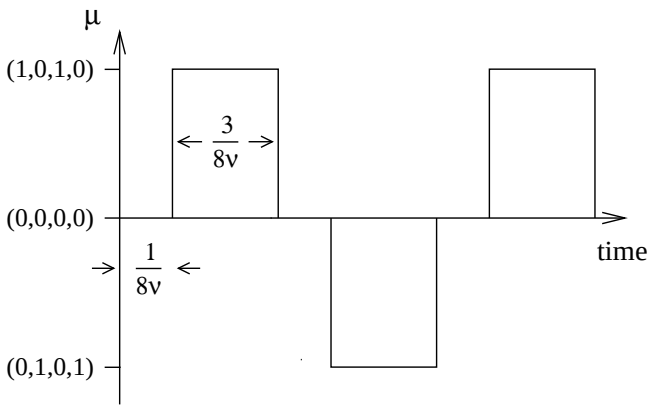

Fig. 2. Stroboscopic alternative motion (SAM). Pattern 1. *Filled circles*, illuminated dots; *open circles*, dots not currently presented. *Left*, vertical motion percept; *right*, horizontal motion percept

2.1 Stroboscopic alternative motion

The traditional stroboscopic alternative motion (SAM) (Hock et al. 1993; Ramachandran and Anstis 1985) uses a quadratic arrangement of dots (Fig. 2). The stimulation consists of two alternating patterns separated by a pause, each pattern consisting of two dots on the same diagonal. An observer perceives succession at low frequency, simultaneity at high frequency, and a motion percept at intermediate frequency. The motion percept is either a vertical motion of two dots or a horizontal motion of two dots, i.e., SAM. On a longer time scale, the motion percept switches from horizontal to vertical and vice versa (Hock et al. 1993); more generally, however, in the vicinity of the abovementioned singularity, the percept switching time may become arbitrarily short.

2.2 Circular apparent motion

Kruse and Stadler (1995b) arranged dots equidistantly on a circle. The first, third and fifth dots, etc., are elicited in the first pattern, while the second, fourth and sixth dots, etc., are elicited in the second pattern. When the patterns alternate with an intermediate frequency, an observer perceives one of two bistable stroboscopic alternative motion percepts, namely either a clockwise or a counter-clockwise circular motion of dots. While this so-called circular apparent motion (CAM) is quite similar to the above SAM, one obtains a richer phenomenology at singular stimulation conditions that give rise to large susceptibilities.

3 Network model

In this and the following sections, a network model is established and analyzed for the particular case of SAM; this model is transferred to the case of CAM as well as to quite general stimulus binding later. A neural network usually has two dynamical rules: the neuronal dynamics models the activity of neurons and the coupling dynamics models the change in synaptic connections (Pineda 1987). In addition, the network architecture and stimulation should be specified for an adapting neural network (Carmesin 1994a).

Notion of couplings. Many neurophysiological and biomolecular events occur at each synapse. In 1949 Hebb proposed the neurophysiological postulate that the efficiency with which a presynaptic neuron can stimulate a postsynaptic neuron increases whenever the presynaptic neuron stimulates the postsynaptic neuron successfully. Inherent in this postulate is the replacement of neurophysiological and biomolecular events at each synapse by an abstract synaptic efficiency. Such an abstract synaptic efficiency is usually called a coupling. In the present paper (Carmesin 1994b), the synaptic efficiency is composed of two factors: a prestabilized factor $\zeta_{ij\delta}$ (modeling slowly changing quantities such as synaptic surface or number of parallel synapses) and a coupling $K_{ij\delta}$ (modeling rapidly changing quantities such as active NMDA receptors). The increase in the fast couplings $K_{ij\delta}$ should be proportional to the slow coupling factors $\zeta_{ij\delta}$ (because these model the prestabilized biomass that takes part in the synaptic modifications) and proportional to the fast couplings $K_{ij\delta}$ (this proportionality is slightly hypothetical in the sense that there is no clear empirical evidence for or against it; it is plausible in the sense that many biomass changes are proportional to the current biomass, for various reasons). Furthermore, the analysis of the network model turns out to be much simpler in terms of the (transformed) couplings $W^2_{ij\delta} = K_{ij\delta}$, because the dynamics exhibits a potential in the space of the couplings $W_{ij\delta}$. Such potentials have been assumed in some synergetics models (e.g., Kruse et al. 1996). Of course, the modeled empirical quantities, such as EEG potentials, are expressed in terms of the original couplings $K_{ij\delta}$ (see, for example, Carmesin 1994b).

Altogether, the binding of two stimuli is instantiated here by the product of a fast and a slow coupling factor. Accordingly, these two factors $K_{ij\delta}$ and $\zeta_{ij\delta}$ are denoted as *binding factors*. The generality of the concept of binding factors is emphasized elsewhere (Carmesin 1994a,b). In this spirit, the present network model (Carmesin 1994a,b) may be denoted as a *binding factor model of perception*. From the point of view of network theory, such stimulus binding is related to neuronal self-organization of topological order (see, for instance, Weiss 1928; Marshall et al. 1941; Willshaw and von der Malsburg 1976; Carmesin 1994c,1996).

3.1 Network architecture

The network architecture is established by N sensor neurons $\hat{n}_j$ and by N inner neurons n_i and by all possible couplings $W_{ij\delta}$ among inner neurons; thus a coupling $W_{ij\delta}$ transfers

$$\begin{array}{ccc} n_1 & \leftrightarrow & n_2 \\ \updownarrow & & \updownarrow \\ n_4 & \leftrightarrow & n_3 \end{array}$$

Fig. 3. Network architecture. Four inner neurons n_1, n_2, n_3, n_4 correspond to four stimulation dots. There are eight possible couplings; some of these emerge according to the network dynamics. The emergent couplings establish binding of successive stimuli; this instantiates a motion percept

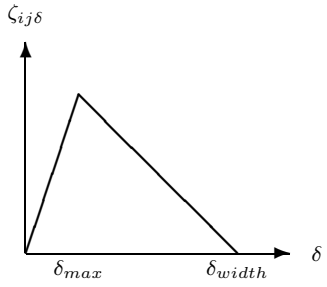

Fig. 4. Prestabilized factors. *Abscissa*, coupling delay time δ. *Ordinate*, prestabilized coupling factor instantiating preferential binding of successive and neighboring stimuli

signals from a neuron n_j at a time step t to a neuron n_i at a time step $t + 1 + \delta$. The sensor neurons are stimulated according to the above SAM (Fig. 1). Altogether the network consists of four sensor neurons and four inner neurons (Fig. 3).

3.2 Network dynamics

Neuronal states. The neurons take values $0/1$ at discrete time steps $t = 1, 2, 3, \ldots$, that is $n_j(t) = 0/1$ and $n_i(t) = n_i = 0/1$. Here and in the following, the time index is omitted if it is t.

Prestabilized coupling factors. This network model uses couplings $W_{ij\delta}$ that change during perception and so-called prestabilized coupling factors $\zeta_{ij\delta}$ that do not change during perception. This concept was introduced in Carmesin (1994b); there and in Carmesin (1994a) it is explicated how the fast couplings $W_{ij\delta}$ might be instantiated by slow couplings; neuroscientifically it is still an open question (the study of which is currently in preparation) whether rapid synaptic modifications are relevant for percept formation.

The prestabilized coupling factors $\zeta_{ij\delta}$ encode *Gestalt laws* (Köhler 1920; Metzger 1975; Carmesin 1994a,b), such as the rule that narrow and subsequent stimuli are bound preferentially. Accordingly, a space factor ζ_{ij} is used with $\zeta_{ij} > \zeta_{km}$ for distance $(\hat{n}_i - \hat{n}_j) >$ distance $(\hat{n}_k - \hat{n}_m)$.

The human nervous system prefers vertical percepts to horizontal percepts. Thus the horizontal and vertical prestabilized factors ζ_h and ζ_v are equal when the four stimuli are arranged as a rectangle with length ratio (alias aspect ratio) equal to 8/5.

Moreover, the preferential binding of subsequent stimuli is expressed with a triangle-type function (Fig. 4)

$$\zeta_{ij\delta} = \zeta_{ij} \begin{cases} \delta/\delta_{\max} & \text{for } 0 < \delta < \delta_{\max}; \\ 1 - \frac{\delta - \delta_{\max}}{\delta_{\text{width}} - \delta_{\max}} & \text{for } \delta_{\max} < \delta < \delta_{\text{width}}; \\ 0 & \text{otherwise} \end{cases} \qquad (1)$$

Here the prestabilized factors are chosen arbitrarily and only for the sake of explicitness. However, there are numerous empirical data about the efficiency of stimulus binding depending on the time interval and on the distance (Korte 1915; Caelli and Finlay 1981). Such stimulus binding efficiencies indicate the values of the actual prestabilized factors $\zeta_{ij\delta}$; more quantitatively, one may adjust the prestabilized factors $\zeta_{ij\delta}$ so that the network generates those stimulus binding efficiencies that are observed empirically; this is beyond the scope of the present study.

Transferred signals. The signals transferred by the couplings are expressed in terms of a local formal field

$$h_i = \hat{n}_i(t-1) - 1 + \frac{1}{2} \sum_{\delta=0}^{\delta=\delta_{\text{width}}} \sum_{j}^{N} \zeta_{ij\delta} W_{ij\delta}^2 (t-1) n_j (t-1-\delta) \qquad (2)$$

That is, the external stimulation is transferred with a coupling with one time step delay and with weight 1, the subtrahend -1 expresses a threshold and inner neurons contribute according to the product of the prestabilized coupling factors and the square of fast couplings. Due to the dependence of h_i on δ_{width}, previous time steps and the stochastic dynamics introduced below (5), the network establishes a δ_{width}-order Markov process. This stochastic process may be expressed in terms of an equivalent first-order Markov process by introducing the following notation

$$n_j^\delta(t) = n_j(t-\delta)\,; \qquad n_j^\delta(t-1) = n_j(t-1-\delta) \qquad (3)$$

So one gets

$$h_i = \hat{n}_i(t-1) - 1 + \frac{1}{2} \sum_{\delta=0}^{\delta=\delta_{\text{width}}} \sum_{j}^{N} \zeta_{ij\delta} W_{ij\delta}^2 (t-1) n_j^\delta (t-1) \qquad (4)$$

Stochastic neuronal dynamics. The inner neurons n_i prefer to fire according to the stimulating local field h_i; however, there is the possibility that the inner neurons fire differently due to random fluctuations. This is formalized by the Boltzmann probability with a *fluctuation parameter* T as follows:

$$P^B(n_i) = \frac{\exp[h_i n_i / T]}{1 + \exp[h_i / T]} \qquad (5)$$

Coupling dynamics. A coupling weight $W_{ij\delta}$ is increased if the presynaptic and postsynaptic firing are in accord. This is modeled as follows:

$$\Delta W_{ij\delta}^{\text{Hebb}} = a W_{ij\delta} \zeta_{ij\delta} n_i n_j^\delta (t-1) \qquad (6)$$

Here, the coupling change $\Delta W_{ij\delta}^{\text{Hebb}}$ is proportional to a *learning parameter* a and to the present coupling $W_{ij\delta}$ (it is typical for biological growth processes that biological matter, like a coupling, increases in proportion to its present weight).

Dynamics of original couplings. The square in the formal field h_i is due to the original couplings $K_{ij\delta}$. Next, it is shown that the coupling growth law takes the same form for the original couplings $K_{ij\delta} = W_{ij\delta}^2$. Using the partial

derivative $\partial K_{ij\delta}/\partial W_{ij\delta} = 2W_{ij\delta}$, one gets $\Delta K_{ij\delta}^{\text{Hebb}} = 2W_{ij\delta}\,\Delta W_{ij\delta}^{\text{Hebb}}$; thus

$$\Delta K_{ij\delta}^{\text{Hebb}} = 2aK_{ij\delta}\zeta_{ij\delta}n_i n_j^{\delta}(t-1) \tag{7}$$

Neuronal resource limit. Moreover, the above coupling dynamics is modeled with the effective constraint that the total coupling weight at a presynaptic neuron n_j is constant. This is formalized in terms of a Euclidean norm and a radius r in coupling space:

$$\sum_{\delta}\sum_{i} W_{ij\delta}^2 = r^2 \tag{8}$$

An analogous relation is introduced for each postsynaptic neuron:

$$\sum_{\delta}\sum_{j} W_{ij\delta}^2 = r^2 \tag{9}$$

These constraints are in agreement with the empirical observation that the connectivity is quite fixed at a neuron (Reichert 1990).

The above effective constraint is achieved roughly by the following additional coupling changes:

$$\Delta W_{ij\delta}^{\text{norm}} = -\frac{\partial V_j^{\text{prenorm}}}{\partial W_{ij\delta}} - \frac{\partial V_i^{\text{postnorm}}}{\partial W_{ij\delta}} \tag{10}$$

with

$$V_j^{\text{prenorm}} = c\Big(\sum_{i}^{N} W_{ij\delta}^2 - r^2\Big)^2$$

and

$$V_i^{\text{postnorm}} = c\Big(\sum_{j}^{N} W_{ij\delta}^2 - r^2\Big)^2 \tag{11}$$

Here c is a constraint parameter which is larger than the learning parameter a. At the potential minimum, the neuronal resource constraints, (8) and (9), are obeyed.

Resource deficits. An essential feature of perception is that a percept becomes unstable after a while. This is modeled here with so-called *resource deficits* X_{ij}. Physiologically, this includes the possibility that the fast couplings decay very rapidly (within 100–1000 ms, for instance); as a result, the stimulus binding may be instantiated by the formation *and* decay of coupling states (that is of networks) within roughly 300 ms.

These resource deficits may be interpreted as a lack of attention or as a lack of relevant neurotransmitters, that is, X_{ij} is a measure for a deficit in metabolic or other resources. A resource deficit X_{ij} diminishes the corresponding fast couplings

$$\Delta W_{ij\delta}^{\text{resource}} = -X_{ij}(t-1) \tag{12}$$

A resource deficit X_{ij} diminishes with time and increases by a corresponding fast coupling 'activity'

$$\Delta X_{ij} = -\alpha_c X_{ij}(t-1) + \beta_c \sum_{\delta} W_{ij\delta}(t-1) \tag{13}$$

Table 1. Model parameters used in the network model

Notation	Parameter	Comment
a	Learning parameter	Network dynamics
T	Fluctuation rate	Network dynamics
c, r	Constraint parameters	Neuronal resource limit
α_c, β_c	Coupling resource parameters	Resource dynamics
ν	Frequency	Stimulation
$\zeta_{ij\delta}$	Prestabilized coupling factor	Codes Gestalt laws

The effect of the present resource deficits on the fast couplings may be expressed in terms of a potential

$$\Delta W_{ij\delta}^{\text{resource}} = -\frac{\partial V_{ij\delta}^{\text{resource}}}{\partial W_{ij\delta}} \tag{14}$$

with

$$V_{ij\delta}^{\text{resource}} = W_{ij\delta}X_{ij} \tag{15}$$

Altogether, the total coupling change is the sum

$$\Delta W_{ij\delta} = \Delta W_{ij\delta}^{\text{Hebb}} + \Delta W_{ij\delta}^{\text{norm}} + \Delta W_{ij\delta}^{\text{resource}} \tag{16}$$

3.3 Model parameter overview

Table 1 gives an overview of model parameters used in the network model. The table indicates that the basic network dynamics of neurons and couplings is specified by two parameters: the learning rate a indicating the velocity of coupling changes and the fluctuation rate T of neuronal fluctuations. It is realistic to assume limited resources at neurons and couplings. These are modeled with simple difference equations and give rise to two parameters for each mechanism; in this manner, four further parameters are plausible. The stimulation is characterized by a frequency ν. The Gestalt laws that narrow and successive stimuli are bound preferentially are modeled (encoded) with corresponding coupling factors $\zeta_{ij\delta}$. Altogether, the proposed network model appears quite straightforward and relatively simple.

4 Field theoretical solution of the network

Overview of the solution method. In order to solve the above network model, one should specify the coupling matrices that emerge as a result of the combined neuronal, coupling and resource deficit dynamics. This is achieved here as follows (for a very detailed description see Carmesina 1994a). First the combined dynamics is identified as taking place in the combined set of states $(\mathbf{n}, \mathbf{W}, \mathbf{X})$ of neuronal states $\{n_i^{\delta}\}$, couplings and resource deficits. This set may be regarded as being embedded in a *vector space* with continuous values for neurons, couplings and resource deficits and with the neuronal space, coupling space and resource deficit space as subspaces. In this state set, the combined dynamics establishes a *Markov process*, by construction. A reasonable assumption of limited coupling resolution is introduced (this assumption is obeyed, for example, by any computer simulation). As a consequence, the process is ergodic. As a further consequence, the averaged changes may be described by a

vector field. The fast neuronal variables may be solved first in a so-called adiabatic limit. The remaining coupling and resource deficit dynamics is again separated adiabatically, with the coupling dynamics being faster than the resource deficit dynamics. The resulting coupling dynamics for adiabatically fixed resource deficits is characterized by a difference equation that may be derived from a scalar potential. The stationary states of the coupling dynamics are the local potential minima. These stationary states represent the possible emerging networks. As a consequence, the possible emerging networks may be investigated by analyzing the potential minima. The couplings of these emerging networks establish the stimulus binding and thus the emerging percepts. As a result of that analysis one obtains the resulting emerging percepts and their changes due to the slow resource deficit dynamics and due to statistical fluctuations.

4.1 Vector field

Because the combined dynamics is ergodic, it makes sense to characterize the mean changes of combined states in terms of the ensemble average of changes of combined states. This average may be expressed in terms of the conditioned probability $P[\{n_i\}|\{\hat{n}_i(t-1)\},\{n_i^\delta\}(t-1),\mathbf{W}(t-1),T]$ that a neuronal configuration $\{n_i\}$ is taken at the time step t under the condition that at the time step $t-1$ the stimulation is $\{\hat{n}_j(t-1)\}$ and the combined state is $\{n_i^\delta(t)\}(t-1),\mathbf{W}(t)$ and the fluctuation parameter is T. In particular, given that $\mathbf{n}$ specifies $\{n_i^\delta\}$ with $i = 1,2,...,N$ and $\delta = 0,...,\delta_{\text{width}}$ and $P^\mu(t-1)$ specifies the stimulation probability of pattern μ at time $t-1$, this average is the following sum over all possible neuronal events that are relevant for the changes:

$$\langle(\Delta\mathbf{n},\Delta\mathbf{W},\Delta\mathbf{X})\rangle = \sum_{\{\hat{n}_j(t-1)\}}^{2^N} P^\mu(t-1) \sum_{\{n_i^\delta\}}^{2^{N\delta_{\text{width}}}} P^C \times (\Delta\mathbf{n},\Delta\mathbf{W},\Delta\mathbf{X}) \quad (17)$$

with the conditional probability

$$P^C = P[\{n_i^\delta\}|\{\hat{n}_j\}(t-1),\{n_i^\delta\}(t-1),\mathbf{W}(t-1),T] \quad (18)$$

For the sake of explicitness, one may express the above transition probability in detail. For the case $\delta = 0$, the transition probability is equal to the Boltzmann probability P^B (5). For the case $\delta > 0$, the transition probability is of a deterministic type according to (3), that is,

$$n_j^\delta(t) = n_j(t-\delta) = n_j(t-1-(\delta-1)) = n_j^{\delta-1}(t-1) \quad (19)$$

This deterministic probability may be denoted by P^D. Altogether, the above probability may be expressed as a product as follows:

$$P^C = P^B P^D \quad (20)$$

As a consequence, for each T the mean changes $\langle(\Delta\mathbf{n},\Delta\mathbf{W},\Delta\mathbf{X})\rangle$ establish a vector field in the combined space, because such mean changes are functions of the combined state due to the condition of the above conditioned probability and due to the fact that after averaging such mean changes do not depend on the stimulation. This vector field is called a *change field* (Carmesin 1994a).

Adiabatic limits. Typically, the neurons change on the time scale of milliseconds, whereas the coupling change is slightly slower and the resource changes are much slower. Thus one may solve the motion of the fast neurons first by means of an adiabatic limit (that is the leading order of a systematic adiabatic approximation, as described in Haken (1983), and then solve the changes of the slower couplings and resources. Analogously one may solve the couplings secondly and the resource deficits thirdly.

For the purpose of the adiabatic elimination of the fast neuronal degrees of freedom one may proceed as follows (for extensive details see Carmesian 1994a). One may consider a fixed value of the slow couplings and resource deficits and perform the average over the neuronal states (17), and one may use the fact that the state $\{n_i\}$ is generated independently from the state $\{n_i^\delta\}(t-1)$. As a result one obtains for the mean change of couplings the sum over all possible neuronal events relevant for the changes:

$$\langle(\Delta\mathbf{W},\Delta\mathbf{X})\rangle = \sum_{\{\hat{n}_j(t-1)\}}^{2^N} P^\mu(t-1) \sum_{\{n_i^\delta\}}^{2^{N\delta_{\text{width}}}} P^C \times (\Delta\mathbf{W},\Delta\mathbf{X}) \quad (21)$$

Next, one may turn to the adiabatic separation of the couplings from the resource deficits. To this end one may consider adiabatically fixed resource deficits; formally (21) is expressed for fixed X as follows:

$$\langle\Delta\mathbf{W}\rangle = \sum_{\{\hat{n}_j(t-1)\}}^{2^N} P^\mu(t-1) \sum_{\{n_i^\delta\}}^{2^{N\delta_{\text{width}}}} P^C \times (\Delta\mathbf{W}) \quad \text{at fixed } \mathbf{X} \quad (22)$$

These mean coupling changes establish another vector field in coupling space. For the sake of explicitness, one may express the mean coupling change (21) in terms of the components

$$\langle\Delta W_{ij\delta}\rangle = \sum_{\{\hat{n}_j(t-1)\}}^{2^N} P^\mu \sum_{\{n_i^\delta\}}^{2^{2N\delta_{\text{width}}}} P^C \times \Delta W_{ij\delta} \quad \text{at fixed } X_{ij\delta} \quad (23)$$

Whenever a fixed point coupling state $\mathbf{W}^*$ is taken, it gives rise to an adiabatic solution of the resource deficits according to (13):

$$\Delta X_{ij} = -\alpha X_{ij}(t-1) + \beta \sum_\delta W^*_{ij\delta} \quad (24)$$

4.2 Potential field

The mean coupling change in (23) is a vector field in coupling space. Next it is shown that this vector field turns out to be a gradient of a scalar potential, the so-called *change potential* (Carmesin 1994a), that is, a potential field.

Potential theorem. *In the adiabatic limit, the mean coupling change, (23), is the gradient of a scalar potential as follows:*

$$\langle\Delta W_{ij\delta}\rangle = -\frac{\partial V}{\partial W_{ij\delta}} \quad (25)$$

with the scalar potential

$$V = V^{\text{Hebb}} + \sum_{j}^{N} V_j^{\text{prenorm}} + \sum_{i}^{N} V_i^{\text{postnorm}} + \sum_{ij\delta} V_{ij\delta}^{\text{resource}} \quad (26)$$

$$V^{\text{Hebb}} = -aT \sum_{\mu}^{2^N} P^{\mu} \ln Z^{\mu} \quad (27)$$

where the stimulation $\{\hat{n}_j\}$ is denoted by μ and the formal partition functions are

$$Z^{\mu} = \sum_{\{n_i^{\delta}\}}^{2^{N\delta_{\text{width}}}} P^{D} \exp[-H^{\mu}/T] \quad (28)$$

and the formal energy functions are

$$H^{\mu} = -\sum_{i=1}^{N} h_i n_i \qquad \textit{for a fixed stimulation } \mu \quad (29)$$

Accordingly, the stable emerging networks are the local minima of the scalar potential V.

Interpretation of the change potential. The change potential V establishes a synergetic potential function from which the macroscopic phenomena may be derived as below and in Kruse et al. (1996). By construction, the change potential V is neither an energy nor a free energy, because a free energy is defined in equilibrium statistics. In contrast, the change potential V specifies mean changes at nonequilibrium states of open or closed systems. Formally, the change potential is similar to a free energy in the sense that it is a generalization of the free energy for non-equilibrium systems (Carmesin 1995).

Principle underlying the proof. Formally, one may interpret the determination of the potential as an integration; for instance one may integrate (25), so one may get $V = -\int_0^{W_{ij\delta}} \langle \Delta W_{ij\delta} \rangle dW_{ij\delta}$. In this sense the method and the results obtained are *quite general*. The fact that in the particular present case the resulting integral may be expressed in terms of an explicit and *rather simple function* is due to the form of the probability (5) and of the whole network model. In particular, methods of statistical physics are applied here and generalized to the case of single objects such as single neurons and couplings, whereas statistical physics deals with systems in the limit of an infinite number of objects. For the proof see Appendix A.

Interpretation of the potential theorem. The potential V makes possible an intuitive and simple understanding and analysis of the emerging networks in terms of local potential minima. Moreover, one may derive for any desired stimulation (rather than equally distributed as above) the resulting emerging networks. Conversely, one may design for a desired network an appropriate stimulation that gives rise to it.

4.3 Unique binding

Next it is shown that each inner neuron has exactly one presynaptic and one postsynaptic neuron. The conditions for it are stability (this is obeyed in practice) and normalization [this is also obeyed in practice due to the additional dynamics (10)].

Unique binding theorem. *For coupling states that are locally stable with respect to stochastic fluctuations and with respect to variations of the formal temperature T and that obey the normalization constraints: Each inner neuron has exactly one presynaptic inner neuron and one postsynaptic inner neuron.*

Principle underlying the proof. There are two main underlying reasons for the unique binding theorem. First, biological matter does typically grow in proportion to its current biomass; this fact is used for coupling growth here and it is inherent in the factor $W_{ij\delta}$ in the coupling dynamics (6). This gives rise to the fact that large couplings tend to grow faster than small couplings. Second, biological matter does typically grow within certain limits. Such a limit is used at a neuron in a quite local manner and is expressed via the constraints (8) or alternatively via the additional dynamics (10). It is already clear intuitively that the combination of the first and second reasons gives rise to a tendency towards states with one coupling at a neuron. For the proof see Appendix B.

5 Modeling phenomena

5.1 Stroboscopic alternative motion SAM

5.1.1 Emerging couplings

Couplings emerging at a neuron for low and intermediate stimulation frequency. Due to the unique binding theorem, exactly one coupling $W_{ij\delta}$ remains at a postsynaptic neuron n_i. In general, the remaining coupling connects neuronal states n_i and n_j^{δ} that are both nonzero; such states are indicated in Fig. 1. Among such nonzero states, those n_i and n_j^{δ} are connected that have the largest corresponding prestabilized factor $\zeta_{ij\delta}$. At low and intermediate stimulation frequency the emerging coupling has a time delay larger than δ_{max} (Fig. 4). As a result, the emerging coupling $W_{ij\delta}$ has the minimum possible delay, $\delta_{\text{Min}} = 1/8\nu$, because couplings with shorter delay cannot provide a postsynaptic signal to a currently stimulated neuron (Fig. 1). Moreover n_j is a neighbor of n_i. Each neuron n_i has a horizontal neighbor $n_{h(i)}$ and a vertical neighbor $n_{v(i)}$. So, one of two possible nonzero couplings remain at a postsynaptic neuron n_i, namely $W_{i,h(i),\delta_{\text{Min}}}$ and $W_{i,v(i),\delta_{\text{Min}}}$.

Emerging coupling states. Due to the unique binding theorem the network model exhibits four stationary coupling states: vertical, horizontal, clockwise and counterclockwise (Fig. 5). Humans, however, perceive mostly vertical or horizontal percepts.

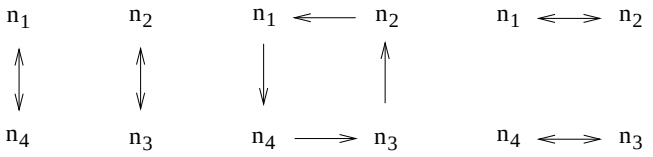

Fig. 5. Emerging networks. *Arrows* indicate emergent couplings and thus motion of dots in the generated motion percept. *Left*, vertical percept; *middle*, circular counter-clockwise percept (circular clockwise percept omitted in figure); *right*, horizontal percept

A possible explanation is a follows. Circular percepts are stable only for $\zeta_h = \zeta_\mathrm{v}$. If the preference for horizontal percepts in humans is provided by a different system, that is not by the present network, then that different system generates a vertical percept preference at $\zeta_h = \zeta_\mathrm{v}$ and the network provides a non-circular preference at $\zeta_h \neq \zeta_\mathrm{v}$. So there remains no stimulation with stable circular percepts.

As a consequence, only two coupling states remain (Fig. 5). In one coupling state, all couplings are horizontal: $W_{i,h(i),\delta_\mathrm{Min}} \neq 0$. In the other coupling state, all couplings are vertical: $W_{i,v(i),\delta_\mathrm{Min}} \neq 0$. Due to the symmetry of the stimulation and of the network, all vertical couplings $W_{i,v(i),\delta_\mathrm{Min}}$ are equal and all horizontal couplings $W_{i,h(i),\delta_\mathrm{Min}}$ are equal.

For the purpose of an illustrative analysis, the emerging coupling state is formally expressed in terms of a linear combination of these two possible states. So the remaining problem is two-dimensional. The decision between horizontal and vertical emerging couplings may be expressed by the angle variable in a polar coordinate system. That is,

$$W_{i,h(i),\delta_\mathrm{Min}} = \rho\cos\phi; \qquad W_{i,v(i),\delta_\mathrm{Min}} = \rho\sin\phi \tag{30}$$

Resource deficit dynamics in terms of polar coordinates. One may derive the resource changes by inserting (30) into (13), so that one gets

$$\begin{aligned}\Delta X_{i,h(i),\delta_\mathrm{Min}} &= -\alpha_c X_{i,h(i),\delta_\mathrm{Min}} + \beta_c\rho\cos\phi\\ \Delta X_{i,v(i),\delta_\mathrm{Min}} &= -\alpha_c X_{i,v(i),\delta_\mathrm{Min}} + \beta_c\rho\sin\phi\end{aligned} \tag{31}$$

Next one may derive the corresponding coupling changes by inserting (30) into (12), so that one obtains

$$\begin{aligned}\Delta W^{\mathrm{resource}}_{i,h(i),\delta_\mathrm{Min}}(t) &= -X_{i,h(i),\delta_\mathrm{Min}}(t-1)\\ \Delta W^{\mathrm{resource}}_{i,v(i),\delta_\mathrm{Min}}(t) &= -X_{i,v(i),\delta_\mathrm{Min}}(t-1)\end{aligned} \tag{32}$$

This coupling change may be expressed in terms of a potential

$$\Delta W_{i,h(i),\delta^{\mathrm{resource}}_\mathrm{Min}} = -\frac{\partial V^{\mathrm{resource}}}{\partial W_{i,h(i),\delta_\mathrm{Min}}} \tag{33}$$

and

$$\Delta W_{i,v(i),\delta^{\mathrm{resource}}_\mathrm{Min}} = -\frac{\partial V^{\mathrm{resource}}}{\partial W_{i,v(i),\delta_\mathrm{Min}}} \tag{34}$$

with

$$V^{\mathrm{resource}} = W_{i,h(i),\delta_\mathrm{Min}} X_{i,h(i),\delta_\mathrm{Min}} + W_{i,v(i),\delta_\mathrm{Min}} X_{i,v(i),\delta_\mathrm{Min}} \tag{35}$$

The above potential may be explained in terms of polar coordinates.

$$V^{\mathrm{resource}} = \rho\cos\phi X_{i,h(i),\delta_\mathrm{Min}} + \rho\sin\phi X_{i,v(i),\delta_\mathrm{Min}} \tag{36}$$

5.1.2 Complete continuous dynamics

Next one may express the dynamics in terms of differential quotients instead of difference quotients. Moreover one may abbreviate $X_{i,h(i),\delta_\mathrm{Min}}$ by X_h and $X_{i,v(i),\delta_\mathrm{Min}}$ by X_v. So one gets the full continuous dynamics in terms of the following system of coupled differential equations [formally this is obtained from (13), (23) and (26) via the transformation of (30)]:

$$\begin{aligned}\frac{\partial\rho}{\partial t} &= -\frac{\partial V}{\partial\rho}\\ \frac{\partial\phi}{\partial t} &= -\frac{\partial V}{\partial\phi}\\ \frac{\partial X_h}{\partial t} &= -\alpha_c X_h + \beta_c\rho\cos\phi\\ \frac{\partial X_\mathrm{v}}{\partial t} &= -\alpha_c X_\mathrm{v} + \beta_c\rho\sin\phi\end{aligned} \tag{37}$$

with

$$V = V^{\mathrm{Hebb}} + V^{\mathrm{norm}} + V^{\mathrm{resource}}$$

and

$$V^{\mathrm{resource}} = \rho\cos\phi\ X_h + \rho\sin\phi\ X_\mathrm{v} \tag{38}$$

The two potentials V^{Hebb} and V^{norm} are specified further in (48) to (56).

5.1.3 Continuous phase transition

Explicit form of the potential V^{Hebb} in the $W_{i,h(i),\delta_\mathrm{Min}}$–$W_{i,v(i),\delta_\mathrm{Min}}$ plane for the case of relatively small prestabilized couplings. Because the only candidates for nonzero couplings are $W_{i,h(i),\delta_\mathrm{Min}}$ and $W_{i,v(i),\delta_\mathrm{Min}}$, the formal local field (2) takes the form

$$\begin{aligned}h_i = \hat{n}_i(t-1) - 1\\ + \frac{1}{2}\zeta_{i,h(i),\delta_\mathrm{Min}} W^2_{i,h(i),\delta_\mathrm{Min}}(t-1) n_{h(i)}(t-1-\delta_\mathrm{Min})\\ + \frac{1}{2}\zeta_{i,v(i),\delta_\mathrm{Min}} W^2_{i,v(i),\delta_\mathrm{Min}}(t-1) n_{v(i)}(t-1-\delta_\mathrm{Min})\end{aligned} \tag{39}$$

Only three stimulation patterns μ occur with nonzero probability P^μ, namely $\mu = 1$: $(\hat{n}_1, \hat{n}_2, \hat{n}_3, \hat{n}_4) = (1, 0, 1, 0)$, $\mu = 2$: $(0, 1, 0, 1)$ and $\mu = 3$: $(0, 0, 0, 0)$. The corresponding probabilities P^μ are (Fig. 1)

$$P^\mu = \frac{1}{3} \qquad \text{for } \mu = 1, 2, 3 \tag{40}$$

In the case being considered of relatively small prestabilized couplings, a neuron n_i can in practice only fire if the corresponding sensor neuron fired at the previous time step, that is if $\hat{n}_i(t-1) = 1$. In this case the threshold -1 cannot be overcome without $\hat{n}_i(t-1) = 1$. For the sake of simplicity one may express this as follows [for $\hat{n}^\mu_i(t-1) = 1$]:

$$\begin{aligned}h^\mu_i = \frac{1}{2}\zeta_{i,h(i),\delta_\mathrm{Min}} W^2_{i,h(i),\delta_\mathrm{Min}}(t-1) n_{h(i)}(t-1-\delta_\mathrm{Min})\\ + \frac{1}{2}\zeta_{i,v(i),\delta_\mathrm{Min}} W^2_{i,v(i),\delta_\mathrm{Min}}(t-1) n_{v(i)}(t-1-\delta_\mathrm{Min})\\ h^\mu_i = -\infty \text{ otherwise}\end{aligned} \tag{41}$$

As a consequence, the formal energy for pattern 1 is obtained from $n_2 = n_4 = 0$ and by inserting (39) into (29) for $i = 1, 3$. So one gets:

$$\begin{aligned} H^1 = & -n_1[\zeta_{i,h(i),\delta_{\text{Min}}} W^2_{i,h(i),\delta_{\text{Min}}}(t-1) n_2(t-1-\delta_{\text{Min}}) \\ & - \zeta_{i,v(i),\delta_{\text{Min}}} W^2_{i,v(i),\delta_{\text{Min}}}(t-1) n_4(t-1-\delta_{\text{Min}})] \\ & - n_3[\zeta_{i,h(i),\delta_{\text{Min}}} W^2_{i,h(i),\delta_{\text{Min}}}(t-1) n_4(t-1-\delta_{\text{Min}}) \\ & - \zeta_{i,v(i),\delta_{\text{Min}}} W^2_{i,v(i),\delta_{\text{Min}}}(t-1) n_2(t-1-\delta_{\text{Min}})] \end{aligned} \quad (42)$$

Analogously one obtains

$$\begin{aligned} H^2 = & -n_2[\zeta_{i,h(i),\delta_{\text{Min}}} W^2_{i,h(i),\delta_{\text{Min}}}(t-1) n_1(t-1-\delta_{\text{Min}}) \\ & - \zeta_{i,v(i),\delta_{\text{Min}}} W^2_{i,v(i),\delta_{\text{Min}}}(t-1) n_3(t-1-\delta_{\text{Min}})] \\ & - n_4[\zeta_{i,h(i),\delta_{\text{Min}}} W^2_{i,h(i),\delta_{\text{Min}}}(t-1) n_3(t-1-\delta_{\text{Min}}) \\ & - \zeta_{i,v(i),\delta_{\text{Min}}} W^2_{i,v(i),\delta_{\text{Min}}}(t-1) n_1(t-1-\delta_{\text{Min}})] \\ H^3 = & -\infty \end{aligned} \quad (43)$$

To determine the formal partition functions (28) one should determine the probabilities $P^D(n_i, n_j)$ for the neuronal configurations of $n_i(t-1-\delta_{\text{Min}})$ and $n_j(t-1-\delta_{\text{Min}})$ for the stimulation pattern μ at time t while the other states $\{n_i^\delta\}$ are irrelevant due to zero couplings $W_{ij\delta}$ (30). So one gets $Z^\mu = 0$ for $\mu = 3$ and

$$Z^1 = \sum_{\substack{n_2(t-1-\delta_{\text{Min}}),\\ n_4(t-1-\delta_{\text{Min}})}}^{4} P^D(n_2, n_4) \sum_{n_1, n_3}^{4} \exp[H^1/T] \quad (44)$$

Because we are interested in the phase transition dynamics, the probabilities $P^D(n_i, n_j)$ are not essential here; for simplicity one may thus approximate these as being equal, that is by $\frac{1}{4}$. So one gets

$$\begin{aligned} Z^1 &= \frac{1}{4} \sum_{\substack{n_2(t-1-\delta_{\text{Min}})\\ n_4(t-1-\delta_{\text{Min}})}}^{4} \sum_{n_1, n_3}^{4} \exp[H^1/T] \\ Z^2 &= \frac{1}{4} \sum_{\substack{n_1(t-1-\delta_{\text{Min}})\\ n_3(t-1-\delta_{\text{Min}})}}^{4} \sum_{n_2, n_4}^{4} \exp[H^2/T] \end{aligned} \quad (45)$$

Inserting (42) and (43) and expanding the 16 possible configurations, yields:

$$\begin{aligned} Z^1 = Z^2 = \frac{1}{4}\Big(& 7 + 2\exp[\zeta_{i,h(i),\delta_{\text{Min}}} W^2_{i,h(i),\delta_{\text{Min}}}(t-1)/T] \\ & + 2\exp[\zeta_{i,v(i),\delta_{\text{Min}}} W^2_{i,v(i),\delta_{\text{Min}}}(t-1)/T] \\ & + 4\exp[\zeta_{i,h(i),\delta_{\text{Min}}} W^2_{i,h(i),\delta_{\text{Min}}}(t-1)/T \\ & + \zeta_{i,v(i),\delta_{\text{Min}}} W^2_{i,v(i),\delta_{\text{Min}}}(t-1)/T] \\ & + \exp[2\zeta_{i,h(i),\delta_{\text{Min}}} W^2_{i,h(i),\delta_{\text{Min}}}(t-1)/T \\ & + 2\zeta_{i,v(i),\delta_{\text{Min}}} W^2_{i,v(i),\delta_{\text{Min}}}(t-1)/T]\Big) \end{aligned} \quad (46)$$

Next one may use polar coordinates:

$$\begin{aligned} Z^1 = Z^2 = \frac{1}{4}\Big(& 7 + 2\exp[\rho^2 \zeta_{i,h(i),\delta_{\text{Min}}} \cos^2\phi/T] \\ & + 2\exp[\rho^2 \zeta_{i,v(i),\delta_{\text{Min}}} \sin^2\phi/T] \\ & + 4\exp[\rho^2(\zeta_{i,h(i),\delta_{\text{Min}}} \cos^2\phi \\ & + \zeta_{i,v(i),\delta_{\text{Min}}} \sin^2\phi)/T] \\ & + \exp[\rho^2(2\zeta_{i,h(i),\delta_{\text{Min}}} \cos^2\phi \\ & + 2\zeta_{i,v(i),\delta_{\text{Min}}} \sin^2\phi)/T]\Big) \end{aligned} \quad (47)$$

So the potential V^{Hebb} is (27) up to an irrelevant term $\ln 4$ and due to $P^\mu = 1/3$ (40):

$$\begin{aligned} V^{\text{Hebb}} = -\frac{aT}{3} \ln\Big(& 7 + 2\exp[\rho^2 \zeta_{i,h(i),\delta_{\text{Min}}} \cos^2\phi/T] \\ & + 2\exp[\rho^2 \zeta_{i,v(i),\delta_{\text{Min}}} \sin^2\phi/T] \\ & + 4\exp[\rho^2(\zeta_{i,h(i),\delta_{\text{Min}}} \cos^2\phi \\ & + \zeta_{i,v(i),\delta_{\text{Min}}} \sin^2\phi)/T] \\ & + \exp[\rho^2(2\zeta_{i,h(i),\delta_{\text{Min}}} \cos^2\phi \\ & + 2\zeta_{i,v(i),\delta_{\text{Min}}} \sin^2\phi)/T]\Big) \end{aligned} \quad (48)$$

Lower limit frequency. For sufficiently low stimulation frequencies ν, one gets $\zeta_{i,j,\delta_{\text{Min}}} = 0$ (Fig. 4). Then there occurs a zero coupling product $\zeta_{i,j,\delta_{\text{Min}}} W^2_{i,j,\delta_{\text{Min}}}$, so no stimulus binding and no motion percept occurs. The limit frequency is determined as follows.

Potential V at small couplings. For small prestabilized coupling factors $\zeta_{ij\delta}$ one obtains small couplings $W_{ij\delta}$. So it is adequate to consider a power series expansion up to the order 4 of the potential V; this is the essence of so-called Ginzburg-Landau theory (Landau and Lifschitz 1979). Here one may first consider fixed resource deficits. Up to fourth order in the couplings, the potential V^{Hebb} takes the form

$$\begin{aligned} V^{\text{Hebb}} = -\frac{a\rho^2}{6}\Big[& \zeta_{i,h(i),\delta_{\text{Min}}} \cos^2\phi + \zeta_{i,v(i),\delta_{\text{Min}}} \sin^2\phi \\ & + \frac{3}{8}\frac{\rho^2}{T}\zeta^2_{i,h(i),\delta_{\text{Min}}} \cos^4\phi + \frac{3}{8}\frac{\rho^2}{T}\zeta^2_{i,v(i),\delta_{\text{Min}}} \sin^4\phi \\ & + \frac{\rho^2}{2T}\cos^2\phi \sin^2\phi\, \zeta_{i,h(i),\delta_{\text{Min}}} \zeta_{i,v(i),\delta_{\text{Min}}}\Big] \end{aligned} \quad (49)$$

Due to the emergence of two couplings (30), the normalization potentials (10) take the form

$$V_i^{\text{prenorm}} = V_j^{\text{postnorm}} = c(\rho^2 - r^2)^2 \quad (50)$$

Up to the irrelevant constant $c^2 r^4$, the sum of these potentials takes the form

$$\begin{aligned} V^{\text{norm}} &= \sum_i^N V_i^{\text{prenorm}} + \sum_j^N V_j^{\text{postnorm}} \\ &= 2Nc\rho^4 - 4r^2 Nc\rho^2 \end{aligned} \quad (51)$$

Thus at fixed resource deficits, the potential takes the form

$$V = V^{\text{Hebb}} + V^{\text{norm}} = (A_1 - A_2)\rho^2 + (B_1 - B_2)\rho^4 \quad (52)$$

with abbreviations

$$\begin{aligned} A_1 &= -4Ncr^2 \\ A_2 &= \frac{a}{6}[\zeta_{i,h(i),\delta_{\text{Min}}} \cos^2\phi + \zeta_{i,v(i),\delta_{\text{Min}}} \sin^2\phi] \\ B_1 &= 2Nc \\ B_2 &= \frac{3}{8T}\zeta^2_{i,h(i),\delta_{\text{Min}}} \cos^4\phi + \frac{3}{8T}\zeta^2_{i,v(i),\delta_{\text{Min}}} \sin^4\phi \\ & \quad + \frac{1}{2T}\cos^2\phi \sin^2\phi\, \zeta_{i,h(i),\delta_{\text{Min}}} \zeta_{i,v(i),\delta_{\text{Min}}} \end{aligned} \quad (53)$$

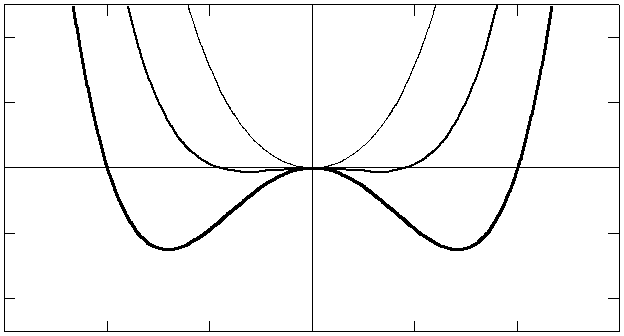

Fig. 6. Continuous phase transition. *Abscissa*, order parameter radius ρ; *ordinate*, potential V at fixed order parameter angle ϕ. Local minima occur at fixed ϕ locally stable order parameter radius ρ. *Upper curve*, prestabilized couplings ζ below critical value ζ_c with $\rho = 0$ (no stimulus binding). *Middle curve*, ζ slightly above ζ_c with small but nonzero order parameter radius $\rho \neq 0$. *Lower curve*, ζ above ζ_c with nonzero order parameter radius $\rho \neq 0$. Continuous phase transition: the stable order parameter radius ρ changes continuously as a function of the parameter A, that is of ζ

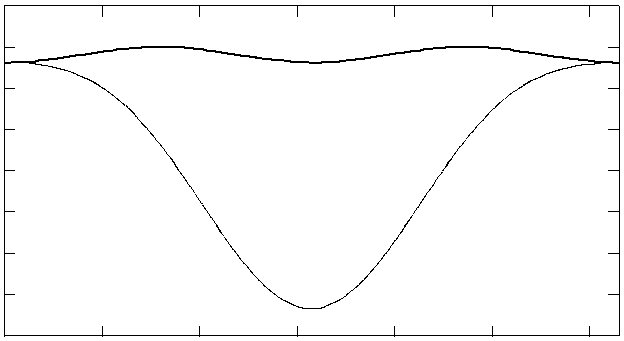

Fig. 7. Disambiguation. *Abscissa*, order parameter angle ϕ; *ordinate*, potential V^{Hebb} at fixed nonzero order parameter radius ρ. Local minima occur at fixed ρ locally stable order parameter angle ϕ. *Upper curve*, equal prestabilized factors for horizontal and vertical couplings yield equally stable horizontal and vertical percepts. *Lower curve*, prestabilized horizontal coupling factor twice as large as vertical coupling factor yields stable horizontal percept only. Result: no mixed percepts emerge (disambiguation)

This potential is the basis for the phase transition scenario according to Ginzburg-Landau theory (Landau and Lifshitz 1979) as follows. The complete set of differential equations is given in Appendix C.

Phase transition scenario. For positive abbreviation parameter $A = A_1 - A_2$, the potential has one minimum at $\rho = 0$, that is, no couplings emerge, hence no percept is generated. At $A = 0$ there occurs a continuous phase transition. The order parameters are characterized in the ρ-ϕ plane. For simplicity, one may study the dependences separately.

For any fixed angle, one gets the classical scenario of a continuous phase transition at $A = 0$. This may be analyzed quantitatively as follows. In accordance with the unique binding theorem, the locally stable states are at $\phi = 0$ or at $\phi = \pi/2$. So it suffices at the phase transition to consider the larger of the two prestabilized factors in A_2, which may be denoted by ζ; the corresponding $\cos^2$ or $\sin^2$ is 1. Thus at the transition, A_2 takes the form

$$A_2 = \frac{a}{6}\zeta \tag{54}$$

Hence the critical prestabilized coupling factor is

$$\zeta_c = \frac{6}{a}A_1 \tag{55}$$

Thus the abbreviation parameter A takes the form

$$A = \frac{a}{6}(\zeta_c - \zeta) \tag{56}$$

The prestabilized coupling ζ may be varied according to the frequency ν, for instance (Fig. 4); this yields the phase transition scenario of Fig. 6.

For any nonzero fixed radius ρ one gets one or two local minima: one corresponding to a vertical percept, one corresponding to a horizontal percept (Fig. 7).

5.2 Circular apparent motion

5.2.1 Network theory

The case of the CAM can be treated analogously. The network model is established by one inner neuron n_i and one sensor neuron $\hat{n}_i$ for each stimulus dot. For instance, eight stimulus dots are positioned equidistantly on a circle (Kruse et al. 1995). There are eight corresponding inner neurons. Any two neurons are connected with a coupling including a prestabilized coupling factor. The prestabilized coupling factors, the neuronal dynamics and the coupling dynamics are as above.

The properties of the network model can be analyzed by using the general potential and binding theorems. In accordance with the unique binding theorem, each inner neuron is connected to exactly one other inner neuron in the emerging cell assembly. Moreover, this other inner neuron is a neighboring neuron, following Gestalt laws (see Sect. 3.2). So there remain just two locally stable coupling states, one of which binds the stimuli in clockwise order, the other in counter-clockwise order.

5.2.2 Resulting phenomena

Succession at low frequency. At low frequency, the radius order parameter (Fig. 6) is zero, so no motion percept occurs.

Oscillation at frequencies near the critical frequency of the continuous phase transition. In the vicinity of the continuous phase transition, the potential barrier that separates coupling states with clockwise and counter-clockwise motion percepts is very low. In addition, the current coupling state becomes increasingly destabilized due to the limitation of coupling resources. When the next stimulation occurs, this state is already destabilized, due to the low potential barrier, so the other motion percept is realized. Overall, the motion percept oscillates. This is the same as the percept of oscillating dots. So the resulting percept is ‘dot oscillation’, or so-called fluttering. This phenomenon is particularly interesting because it shows that the potential barrier can be overcome in a completely deterministic manner. While this is remarkable in itself, it allows in addition efficient quantitative experiments.

CAM at high frequency. When the frequency is well above the critical frequency, then the potential barrier separating cell assemblies of clockwise and counter-clockwise percepts is high. Thus the limitation of coupling resources destabilizes the current state so slowly that several stimulations occur before the percept switches. The motion percept therefore occurs with a hysteresis phenomenon (Kruse et al. 1995; and analogously in Hock et al. 1993). Overall, from this point of view, the oscillation corresponds to a (deterministic) tendency to avoid the old state at the next stimulation, whereas the hysteresis corresponds to a tendency to remain at the old state at the next stimulation; oscillation and hysteresis are thus two aspects of the same phenomenon – the negative or positive correlation with the old state.

6 Discussion

Continuous phase transition. By definition, a phase transition is called *continuous* if the order parameter increases continuously as a function of the control parameter.

For the case of vanishing resource deficits X_{ij} and equal preference for the vertical and orthogonal percept, that is $\zeta_{\mathrm{v}} = \zeta_h$, the two-dimensional order parameter (ϕ, ρ) is (0,0) at the transition ζ_c; furthermore, for increasing ζ the two-dimensional order parameter (ϕ, ρ) becomes nonzero as a continuous function of the coupling ζ. Thus a continuous phase transition occurs. The control parameter of this continuous phase transition is not uniquely determined; instead there are several possible choices: for instance one may increase the prestabilized couplings, decrease the temperature, or increase the stimulation frequency. The last choice is realized in the experiments (Kruse et al. 1996).

For the case of nonvanishing resource deficits X_{ij} with the introduced resource dynamics, the two-dimensional order parameter (ϕ, ρ) is again (0,0) at the transition ζ_c and again the two-dimensional order parameters (ϕ, ρ) increase continuously for increasing prestabilized couplings ζ. *So the phase transition remains continuous.*

For the sake of a complete discussion, it is added here that the phase transition does have several properties that are usually common to discontinuous phase transitions: the potential function V becomes asymmetric when the resource deficits become asymmetric $X_h \neq X_{\mathrm{v}}$, the angle component ϕ of the order parameter varies discontinuously. However, the essential point is that this is only due to the singular behavior of polar coordinates in the vicinity of the pole; the actual two-dimensional order parameter change remains infinitesimal, as does the potential barrier ΔV.

Scenario at high stimulation frequency. Due to the decrease in prestabilized coupling factors for short time alias high stimulation frequency (Fig. 4), a similar continuous phase transition occurs at high stimulation frequency; such a transition is observed experimentally. In principle, there may occur additional percepts at high stimulation frequency, due to the fact that the prestabilized factor for the binding of successive stimuli may become smaller than that for the binding of nonsuccessive stimuli. Corresponding effects may be observed in a film of a spoked wheel rotating: at low velocity the spokes are perceived as rotating in the same direction as the wheel, while the opposite direction is perceived at appropriately high velocity.

Comparison with experiments. The indicated phenomena are in agreement with psychophysical experiments (Kruse et al. 1996). Further experiments concerning critical exponents and fluctuations at the continuous transition are currently in progress and in preparation. Moreover, the low change potential barrier at the continuous transition gives rise to sensitive measurement conditions; these might be advantageous for experiments concerning underlying psychophysical mechanisms.

7 Physiological models for fast couplings

So far, the neural network has been used to model psychological and physiological empirical findings about perception. The neuronal dynamics and the coupling dynamics are thus biologically quite plausible, due to the neuronal fluctuations and due to the Hebb rule.

Each of the neurons modeled here for a single stimulus dot is considered to correspond to various nerve cells, presumably distributed in various cortical maps and areas.

As discussed at the beginning of the network model, Hebbian coupling is, by definition (Hebb 1949), an abstract and effective quantity, the physiological and molecular basis of which has to be investigated (Brown et al. 1990; Kandel et al. 1991). Here the possible neuronal instantiation of fast Hebbian couplings is discussed in more detail (Flohr 1991, 1994). According to a possible mechanism elaborated in Carmesin (1994a,b), fast couplings might be instantiated by small subnetworks indirectly. It is, however, also possible that fast couplings are instantiated directly on the basis of appropriate neuro-transmitters, a popular candidate being the NMDA mechanism (Flohr 1991, 1994). The fast formation of couplings has already been proposed by von der Malsburg Willshaw and von der Malsburg 1976, Flohr 1991. Here it is suggested that fast couplings do form *and* decay rapidly, according to the modeling of the EEG data (Carmesin 1994a,b). On the basis of the present experimental and theoretical work, one may determine perception order parameters quite precisely in the vicinity of a continuous phase transition; in particular, stochastic effects become relatively small in comparison with the coupling resource effects and the neuronal resource effects. As a result, the effect of possible fast couplings may be studied quantitatively with relatively high precision. Accordingly, the effect of neuropharmacological variations of possible fast couplings on perception order parameters could be investigated quantitatively in future experiments.

8 Conclusion

A general neuronal network model for stimulus binding during perception (Carmesian 1994a,b) is extended, improved and analyzed. The network is characterized by *fast plastic*

couplings, prestabilized coupling factors, slow resource dynamics and by very fast stochastic neuronal dynamics. The fast and prestabilized coupling factors are essential for stimulus binding, so they are called binding factors and the network model is denoted as the *binding factor model of perception.*

General analytic results are derived in the framework of a field theory; in particular, a *potential* that characterizes the dynamics is derived explicitly and it is shown that ambiguous stimulus configurations are *disambiguated*. The present theory is based on the Hebb rule, is physiologically plausible and may be understood as a special case of a more general theory of neuronal adaptation; accordingly, quantitative comparisons of learning and perception are possible (Carmesin 1994a). Structurally, the present network provides a straightforward system for the instantiation of psychological Gestalt laws, due to the prestabilized coupling factors.

For prototypical stimulus sequences, various *phenomena* are derived. Many of these phenomena are reported in Kruse et al. (1996). Thus a *continuous phase transition* is obtained and characterized by a two-dimensional order parameter, one component of which varies continuously and describes a high susceptibility for external stimuli, while the other component varies discontinuously and provides the disambiguation necessary for perception. At the continuous phase transition, the slow resource dynamics becomes relevant and gives rise to the new phenomenon of fluttering.

Experiments (Kruse et al. 1996) confirm the modeled continuous transition, the fluttering including the deterministic percept oscillations, the change potential landscape including its variation with the control parameter; the resulting disambiguation, preferential binding of narrow stimuli (Gestalt law) and hysteresis (Hock et al. 1993); and the qualitative dynamics of the EEG brain potentials in the form of P300 signals (Basar-Eroglu et al. 1993).

Due to the high sensitivity, the continuous phase transition is *advantageous for experiments*. Current and planned experiments include EEG measurement of critical fluctuations, quantitative determination of network parameters from measurements of hysteresis loops, order parameter variation in psycho-pathological persons, and order parameter variation as a function of psychopharmaceutical application.

From a theoretical point of view, continuous phase transitions are advantageous for the following reason: at the continuous transition there occurs a singularity; as a result all non-singular mechanisms become irrelevant. The singular mechanisms may be used for a system classification into so-called universality classes and for a detailed study of the relevant dynamics.

Strictly speaking, these additional phenomena relativize the continuity of the transition. Nevertheless, perception phenomena can be investigated empirically at the continuous transition with the high precision typical of continuous phase transitions, thus a diagnostic method might be provided. The area of the hysteresis loop vanishes when approaching the continuous phase transition.

The slow resource dynamics consists of two components: an *amplitude component* modeling the typical P300 EEG signal and a *structural component* modeling the typical loss of attention for old percepts.

The fast couplings may be instantiated either by small subnetworks or by fast neurotransmitters. Experiments that might investigate the *origin of fast stimulus binding* during perception are currently in preparation.

Appendix A. Proof of the potential theorem

Organization of the proof. First the coupling average is transformed successively until a useful form is obtained. Second the potential gradient is transformed successively until a useful form is obtained. Third the two results are identified as being equal.

Part I: Transformation of the coupling average. To begin with, one may take (23) and express the conditioned probability P^C in terms of the product of P^D and P^B, moreover one may express the latter in terms of the probabilities in (5), because this product is the desired probability that a neuronal state $\{n_i\}$ is taken. So one gets

$$\langle \Delta W_{ij\delta} \rangle = \sum_{\{\hat{n}_j\}}^{2^N} P^\mu \sum_{\{n_i^\delta\}}^{2^{N\delta_{\text{width}}}} P^D \prod_{i=1}^{N} P^B \times \Delta W_{ij\delta} \tag{A1}$$

Next one may insert the probabilities according to (5) and express these probabilities in the denominator with the sum of two exponentials. So one gets

$$\langle \Delta W_{ij\delta} \rangle = \sum_{\{\hat{n}_j\}}^{2^N} P^\mu \sum_{\{n_i^\delta\}}^{2^{N\delta_{\text{width}}}} P^D \times \prod_{i=1}^{N} \frac{\exp[h_i n_i/T]}{\sum_{n_i=0/1}^{2} \exp[h_i n_i/T]} \Delta W_{ij\delta} \tag{A2}$$

Here one may express the product in the numerator and in the denominator separately. Thus one obtains

$$\langle \Delta W_{ij\delta} \rangle = \sum_{\{\hat{n}_j\}}^{2^N} P^\mu \sum_{\{n_i^\delta\}}^{2^{N\delta_{\text{width}}}} P^D \times \frac{\prod_{i=1}^{N} \exp[h_i n_i/T]}{\prod_{i=1}^{N} \sum_{n_i=0/1}^{2} \exp[h_i n_i/T]} \Delta W_{ij\delta} \tag{A3}$$

In the numerator, one may express the product of exponentials as an exponential of a sum. In the denominator, one may exchange the product and the sum according to the distributive law, that is, the product of sums over two neuronal values is equal to the sum over neuronal configurations of products. So one gets

$$\langle \Delta W_{ij\delta} \rangle = \sum_{\{\hat{n}_j\}}^{2^N} P^\mu \sum_{\{n_i^\delta\}}^{2^{N\delta_{\text{width}}}} P^D \times \frac{\exp[\sum_{i=1}^{N} h_i n_i/T]}{\sum_{\{n_i\}}^{2^N} \prod_{i=1}^{N} \exp[h_i n_i/T]} \Delta W_{ij\delta} \tag{A4}$$

Next one may identify the formal energy function in the numerator and express the product of exponentials as an exponential of a sum in the denominator. So one gets

$$\langle \Delta W_{ij\delta} \rangle = \sum_{\{\hat{n}_j\}}^{2^N} P^\mu \sum_{\{n_i^\delta\}}^{2^{N\delta_{\text{width}}}} P^D \times \frac{\exp[-H^\mu/T]}{\sum_{\{n_i\}}^{2^N} \exp[\sum_{i=1}^{N} h_i n_i/T]} \Delta W_{ij\delta} \quad \text{(A5)}$$

Now one may identify the formal energy function in the denominator. So one obtains

$$\langle \Delta W_{ij\delta} \rangle = \sum_{\{\hat{n}_j\}}^{2^N} P^\mu \sum_{\{n_i^\delta\}}^{2^{N\delta_{\text{width}}}} P^D \times \frac{\exp[-H^\mu/T]}{\sum_{\{n_i\}}^{2^N} \exp[-H^\mu/T]} \Delta W_{ij\delta} \quad \text{(A6)}$$

Here one may identify the formal partition function in the denominator. So one derives

$$\langle \Delta W_{ij\delta} \rangle = \sum_{\{\hat{n}_j\}}^{2^N} P^\mu \sum_{\{n_i^\delta\}}^{2^{N\delta_{\text{width}}}} P^D \frac{\exp[-H^\mu/T]}{Z^\mu} \Delta W_{ij\delta} \quad \text{(A7)}$$

Part II: Transformation of the potential gradient. For the purpose of a later comparison, one may perform the gradient of the scalar potential V^{Hebb}

$$-\frac{\partial V^{\text{Hebb}}}{\partial W_{ij\delta}} = -a \sum_{\{\hat{n}_j\}}^{2^N} P^\mu \sum_{\{n_i^\delta\}}^{2^{N\delta_{\text{width}}}} P^D \frac{\exp[-H^\mu/T]}{Z^\mu} \frac{\partial H^\mu}{\partial W_{ij\delta}} \quad \text{(A8)}$$

with (4)

$$\frac{\partial H^\mu}{\partial W_{ij\delta}} = \frac{\partial}{\partial W_{ij\delta}} \Big(-\frac{1}{2} \sum_{km} n_k \Big[\hat{n}_k(t-1) + \sum_{\delta'=0}^{\delta=2\delta_{\text{width}}} \zeta_{km\delta'} W_{km\delta'}^2(t-1) n_m^{\delta'}(t-1) \Big] \Big) \quad \text{(A9)}$$

The above partial derivative yields nonzero terms only if the indices of $W_{ij\delta}$ are equal to the corresponding ones of $W_{km\delta'}$. So one gets

$$\frac{\partial H^\mu}{\partial W_{ij\delta}} = -\zeta_{ij\delta} W_{ij\delta}(t-1) n_j^\delta(t-1) n_i \quad \text{(A10)}$$

By comparison of this expression with (6) one obtains

$$\frac{\partial H^\mu}{\partial W_{ij\delta}} = -\Delta W_{ij\delta}^{\text{Hebb}}/a \quad \text{(A11)}$$

Next one may insert this result in (A8), so one gets

$$-\frac{\partial V^{\text{Hebb}}}{\partial W_{ij\delta}} = \sum_{\{\hat{n}_j\}}^{2^N} P^\mu \sum_{\{n_i^\delta\}}^{2^{N\delta_{\text{width}}}} P^D \frac{\exp[-H^\mu/T]}{Z^\mu} \Delta W_{ij\delta}^{\text{Hebb}} \quad \text{(A12)}$$

Part III: Identity of coupling average and potential gradient. By comparison of this expression with (A7) one obtains

$$\langle \Delta W_{ij\delta}^{\text{Hebb}} \rangle = -\frac{\partial V^{\text{Hebb}}}{\partial W_{ij\delta}^{\text{Hebb}}} \quad \text{(A13)}$$

Moreover, due to the fact that the coupling changes $\Delta W_{ij\delta}^{\text{norm}}$ and $\Delta W_{ij\delta}^{\text{resource}}$ may be averaged without effect here, one gets

$$\langle \Delta W_{ij\delta} \rangle = -\frac{\partial V}{\partial W_{ij\delta}} \quad \text{(A14)}$$

q.e.d.

Appendix B. Proof of the unique binding theorem

Organization of the proof. First the essential competition among the couplings is expressed adequately in multidimensional polar coordinates. Second the emerging networks are analyzed as the potential minima by taking the derivatives and by extracting the conditions under which these derivatives vanish.

Proof. One may use multidimensional polar coordinates for the couplings as follows (10):

$$\begin{aligned} W_{ij\delta} &= r \cos\vartheta_{ij\delta} \\ W_{i+1j\delta} &= r \sin\vartheta_{ij\delta} \cos\vartheta_{i+1,j,\delta} \\ W_{ij\delta+1} &= r \sin\vartheta_{ij\delta} \sin\vartheta_{i+1,j,\delta} \cos\vartheta_{i+1,j,\delta+1} \\ &\dots \end{aligned} \quad \text{(B1)}$$

The networks that are locally stable with respect to stochastic fluctuations are specified by the local minima of the potential V. Consequently, the partial derivatives of the potential V with respect to the above angle variables vanish for these networks, that is

$$\frac{\partial V}{\partial \vartheta_{mk\delta}} = 0 \quad \text{(B2)}$$

To determine the form of such a derivative, one may recall that any angular variable $\vartheta_{mj\delta}$ in the potential V occurs in terms of a $\cos^2\vartheta_{mj\delta}$ or in terms of a $\sin^2\vartheta_{mj\delta}$, because the couplings enter the potential in terms of squares [see (5), (B1), (27), (28) and (29)]. Consequently, the derivative of the potential V with respect to such an angular variable $\vartheta_{mj\delta}$ is proportional to $\sin\vartheta_{mj\delta}\cos\vartheta_{mj\delta}$, in accordance with the chain rule. That is, each such derivative is of the form

$$\frac{\partial V}{\partial \vartheta_{mj\delta}} = \sin\vartheta_{mj\delta}\cos\vartheta_{mj\delta} rest(T) = 0 \quad \text{(B3)}$$

whereby $rest(T)$ denotes the remaining factor, which is a function of the formal temperature. Consequently, a network that is locally stable with respect to stochastic fluctuations obeys either $\sin\vartheta_{mj\delta}\cos\vartheta_{mj\delta} = 0$ or $rest(T) = 0$. The networks that do not obey $\sin\vartheta_{mj\delta}\cos\vartheta_{mj\delta} = 0$ do obey $rest(T) = 0$; thus they vary with the formal temperature, and hence they are not stable with respect to temperature variations. As a consequence, those networks that are locally stable with respect to stochastic fluctuations and with respect to variations of the formal temperature T do obey $\sin\vartheta_{mj\delta}\cos\vartheta_{mj\delta} = 0$. This implies $\vartheta_{mj\delta} = 0$ or $\vartheta_{mj\delta} = \pi/2$. Thus [see (B1)] $W_{ik\delta}$ is either 0 or r.

Moreover, one may recall the constraints [see (8)] $r^2 = \sum_m \sum_\delta W_{mj\delta}^2$. They imply that at each inner neuron n_j, there is exactly one nonzero coupling $W_{mj\delta} = r$ to another inner neuron.

Analogously, the constraints $r^2 = \sum_j \sum_\delta W_{mj\delta}^2$ [see (8)] imply that at each inner neuron n_m, there is exactly one nonzero coupling $W_{mj\delta} = r$ from another inner neuron. That is, each inner neuron is connected with exactly one presynaptic inner neuron and with exactly one postsynaptic inner neuron. q.e.d.

Appendix C. Complete set of equations

The complete set of differential equations is derived from (37) and (52). One obtains:

$$\begin{aligned}
\frac{\partial \rho}{\partial t} &= 8\,N\,c\,r^2\rho \\
&\quad + \frac{a}{3}\left(\zeta_{i,h(i),\delta_{\text{Min}}}\cos^2\phi + \zeta_{i,v(i),\delta_{\text{Min}}}\sin^2\phi\right)\rho \\
&\quad - 8\,N\,C\,\rho^3 + \frac{3}{2}\,\frac{\zeta_{i,h(i),\delta_{\text{Min}}}^2\cos^4\phi}{T}\,\rho^3 \\
&\quad + \frac{3}{2}\,\frac{\zeta_{i,v(i),\delta_{\text{Min}}}^2\sin^4\phi}{T}\,\rho^3 \\
&\quad + 2\,\frac{\cos^2\phi\,\sin^2\phi\,\zeta_{i,h(i),\delta_{\text{Min}}}\,\zeta_{i,v(i),\delta_{\text{Min}}}}{T}\,\rho^3 \\
&\quad - \cos\phi\,X_h - \sin\phi\,X_{\text{v}} \\
\frac{\partial \phi}{\partial t} &= -\frac{a}{3}\,\zeta_{i,h(i),\delta_{\text{Min}}}\cos\phi\,\sin\phi\,\rho^2 \\
&\quad + \frac{a}{3}\,\zeta_{i,v(i),\delta_{\text{Min}}}\sin\phi\,\cos\phi\,\rho^2 \\
&\quad - \frac{3}{2}\,\frac{\zeta_{i,h(i),\delta_{\text{Min}}}^2\cos^3\phi\,\sin\phi}{T}\,\rho^4 \\
&\quad + \frac{3}{2}\,\frac{\zeta_{i,v(i),\delta_{\text{Min}}}^2\sin^3\phi\,\cos\phi}{T}\,\rho^4 \\
&\quad - \frac{\cos\phi\,\sin^3\phi\,\zeta_{i,h(i),\delta_{\text{Min}}}\,\zeta_{i,v(i),\delta_{\text{Min}}}}{T}\,\rho^4 \\
&\quad + \frac{\cos^3\phi\,\sin\phi\,\zeta_{i,h(i),\delta_{\text{Min}}}\,\zeta_{i,v(i),\delta_{\text{Min}}}}{T}\,\rho^4 \\
&\quad + \rho\,\sin\phi\,X_h - \rho\,\cos\phi\,X_{\text{v}} \\
\frac{\partial X_h}{\partial t} &= -\alpha_c X_h + \beta_c \rho\cos\phi \\
\frac{\partial X_{\text{v}}}{\partial t} &= -\alpha_c X_{\text{v}} + \beta_c \rho\sin\phi \qquad \text{(C1)}
\end{aligned}$$

Acknowledgement. We are grateful for stimulating discussions and collaborations with Hans Flohr, Martin Kreyscher, Peter Kruse, Sandra Müller, Lars Pahlke, Gerhard Roth, Florian Sander, Helmut Schwegler, Michael Stadler and Daniel Strüber.

References

Basar-Eroglu C, Strüber D, Stadler M, Kruse P, Basar E (1993) Multistable visual perception induces a slow positive eeg wave. Int J Neurosci 73: 139–151

Brown TH, Kairiss EW, Keenan CL (1990) Hebbian synapses: biophysical mechanisms and algorithms. Annu Rev Neurosci 13: 475–511

Caelli T, Finlay D (1981) Intensity, spatial frequency, and temporal frequency determinants of apparent motion: Korte revisited. Perception 10: 183–189

Carmesin H-O (1994a) Theorie neuronaler Adaption. Köster, Berlin

Carmesin H-O (1994b) Statistical neurodynamics: a model for universal properties of EEG-data and perception. Acta Phys Slovaca 44: 311–330

Carmesin H-O (1994c) Topological order in networks selforganized through local dynamics. In: Böbel FG, Wagner T (eds) ICASSE Proc Fraunhofer-Gesellschaft, Erlangen, pp 53–60

Carmesin H-O (1995) Neurophysics of adaption. Phys Essays 8(1)

Carmesin H-O (1996) Topology-preservation emergence by the Hebb rule with infinitesimal short-range signals. Phys Rev E 53(1)

Corsi P (1991) The enchanted loom. Oxford University Press, New York

Descartes R (1664) L'Homme. Theodore Girard, Paris

Ditzinger T, Haken H (1989) Oscillations in the perception of ambiguous patterns. Biol Cybern 61: 279–287

Flohr H (1991) Brain processes and phenomenal consciousness. Theory Psychol 1: 245–262

Flohr H (1994) Neue Realitäten – Herausforderung der Philosophie. Akademie Verlag, Berlin

Haken H (1983) Advanced synergetics. Springer, Berlin Heidelberg New York

Hebb DO (1949) The organization of behaviour. Wiley, New York, p 62

Hock HS, Kelso JAS, Schöner GG (1993) Bistability and hysteresis in the organization of apparent motion patterns. J Exp Psychol Hum Percept Perform 19: 63–80

Kandel ER, Schwarz JH, Jessell TM (1991) Principles of neural science. Elsevier, New York

Köhler W (1920) Die physischen Gestalten in Ruhe und im stationären Zustand. Vieweg, Braunschweig

Korte A (1915) A. Korte: Kinematoskopische Untersuchungen. Z Psychol 72: 194–296

Kruse P (1988) Stabilität Instabilität Multistabilität – Selbstorganisation und Selbstreferentialität in kognitiven Systemen. Delphin 6(3): 35–57

Kruse P, Stadler M (eds) (1995a) Ambiguity in mind and nature. (Springer series in synergetics, vol 64) Springer, Berlin Heidelberg New York

Kruse P, Stadler M (1995b) The function of meaning in cognitive order formation. In: Kruse P, Stadler M (eds) Ambiguity in mind and nature. (Springer series in synergetics, vol 64) Springer, Berlin Heidelberg New York

Kruse P, Stadler M, Strüber D (1991) Psychological modification and synergetic modelling of perceptual oscillations. In: Haken H, Koepchen HP (eds) Rhythms in physiological systems. Springer, Berlin Heidelberg New York, pp 299–311

Kruse P, Strüber D, Stadler M (1995) The significance of perceptual multistablility for research on cognitive self-organisation. In: Kruse P, Stadler M (eds) Ambiguity in mind and nature. (Springer series in synergetics, vol 64) Springer, Berlin Heidelberg New York

Kruse P, Carmesin H-O, Pahlke L, Strüber D, Stadler M (1995) Continuous phase transitions in the perception of multistable visual patterns. Biol Cybern 73 (in press)

Landau LD, Lifschitz EM (1979) Lehrbuch der Theoretischen Physik, vol V. Akademie-Verlag, Berlin

Marshall WH, Woolsey CN, Bard P (1941) Observations on inner somatic sensory mechanisms of cat and monkey. J Neurophysiol 4: 1–24

Metzger W (1975) Gesetze des Sehens. Kramer, Frankfurt am Main

Necker LA (1832) The London and Edinburgh Philosophical Magazine and Journal of Science 3: 329

Pineda FJ (1987) Generalization of back-propagation to recurrent neural networks. Phys Rev Lett 59: 2229–2232

Ramachandran VS, Anstis SM (1985) Perceptual organization in multistable apparent motion. Perception 14: 135–143

Reichert H (1990) Neurobiologie. Thieme, Stuttgart

Weiss W (1928) Eine neue Theorie der Nervenfunktion. Naturwissenschaften 16: 626–636

Willshaw DJ, Malsburg C von der (1976) How patterned neural connections can be set up by self-organization. Proc R Soc Lond B 194: 431–445